Al-Nahrain Journal for Engineering Sciences **NJES** 23(3)306-312, 2020
http://doi.org/10.29194/NJES.23030306

Strut and Tie Modelling of Reinforced Concrete Deep Beams Under Static and Fixed Pulsating Loading

Ajibola Ibrahim Quadri

Authors affiliations:
1) Department of Civil Engineering, The Federal University of, Akure-Nigeria.
dgeneral1201@gmail.com

Paper History:

Received: 22nd April 2020

Revised: 29th June 2020

Accepted: 14th Aug. 2020

Abstract

Numerical analysis of the performance of reinforced concrete (RC) deep beam subjected to static and fixed-point pulsating loading at the midpoint has been investigated. Three-dimensional nonlinear finite element model using the Strut and Tie approach was adopted. The damage level under the influence of the applied fixed pulsating loading is higher than the static applied loading, hence early crack was observed because of the stepwise loading in the form of vibration. Although the Strut and Tie approach gave a good estimation of the resistance capacity of the beam, the beam undergo high shear damage when subjected to these two types of loading. Material strength properties, applied loadings and cross-sections adopted are some of the factors that affect the performance of the deep beam.

Keywords: Deep Beam, Fixed Pulsating Load, Static Load, Strut and Tie Model

1. Introduction

Reinforced concrete (RC) structures are subjected to various deterioration such as concrete spalling, cracks, large deformation, rebars rupture, and collapse during their service time. This is caused by environmental and man-made factors; aging of the structures, reinforcing bar corrosion, earthquakes, blasts, overloading, etc. [1]. The behavior of some RC members is dominant under shear failure while some experienced flexural failure or bending. Some parts of RC structures are overestimated with certain accuracy during design, while other parts are designed using the rules of thumb or based on experience. However, all parts of structures are important and must be treated accurately because of the nonlinear behavior of concrete [2]. When the span-to-overall depth ratio of a beam (l/d) equal to 4 or less, or the shear span-to-overall depth ratio of a beam (a/d) is equal or less than two, the beam is termed a deep beam. It is often loaded at the face and supported at the opposite face. Deep beams are qualified by having a shear span-depth ratio (a/d) relatively small Figure 1, [3] thus, their behavior is dominant under shear rather than flexure and their capacity depends on the mode of application of load and supports condition. Many investigations have been conducted on the behavior of a simply supported RC deep beam under static loading [3,4], however, some RC deep beams are under the influence of pulsating loading such as the vibrating machine. Their behaviors are different when compared to the static loading [5].

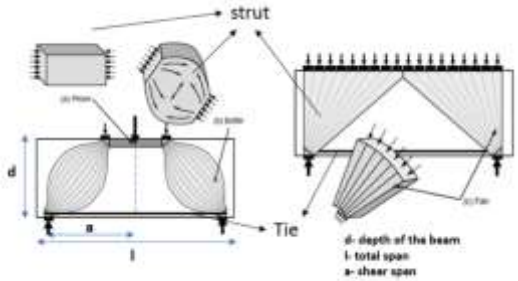

Figure (1): Common types of struts and tie

1.1 Research Significance

Deflection of RC deep beam under static loading is always apparent and allows users to evacuate before the total failure, however, little or no warning is given under the pulsating types of loading. Due to the heterogeneous constituents of concrete, load stress generated under pulsating load is always lower than that of the static stress capacity, thus, crack initiation to propagation may not be apparent before failure. By using the structs-and-ties approach, the bond behavior of the RC beam can easily be analyzed under continuum model. The results of the past

NJES is an **open access Journal** with **ISSN 2521-9154** and **eISSN 2521-9162**

experimental investigations show that the bond-zone response of RC structure is highly nonlinear and always affected by the stress-strain state of the structure [5]. Hence, strut and tie approach is proposed to model the bond strength in the RC deep beam

2. Structs and Ties Consideration

The truss analogy was introduced by Ritter [6], and Morsch [7] more than a century ago, to show the emergence of internal stresses in a cracked beam, which is the basis for the design of concrete beams. This method was improved and extended to be struts and ties by Leonhardt [8], Rusch [9] and Kupfer [10]. Thereafter, Collins and Mitchell, [11] further investigated the deformation of the truss model and came up with a refined approach for shear and torsion. Demerdash, [12] considered a nonlinear finite element approach to design the behavior of deep beam, it was reported that cracking patterns, deflections, failure mode, and stress-strain distributions, cannot be determined with the strut-and-tie model.

Strut and Tie models (STM) are one of the approaches to describe stress growth and distribution developed in a continuum structural field. The action of external loading resulting in flexure, shear, compression, torsion is initially borne by the material constituents in the microscopic level, the overall effect is visible as a failure because once the material is completely in the plastic region, relatively low additional resistance to increase loading is exhibited.

Strut and Tie models are basically a truss analogy that essentially depends on the limit analysis of the lower bound theorem of collapsed load [13]. In this case, only the equilibrium and the yield criterion are satisfied with stress generalization. Hence, in reinforced concrete structures, members subjected to compression termed as Struts are the concrete. The strut transfers stresses from node to other nodes and may be reinforced as structural elements or a typical wall. While the members in tension consist of the steel reinforcement are the Ties that transfer tensile stresses to the nodes. On many cases, transverse reinforcement is provided to prevent the splitting of the RC caused by transverse tension due to the high compressive stress generated by the struts. The shape of the strut depends upon the stress path from which the strut emerges, and details of any tension joined to the tie, [14]. Struct are classified into three as shown in Figure 1, **Prismatic** structs are mainly adopted to model the compressive stress block of a beam member. When the section at the end of the strut is well defined but the rest of the struct is not confined to a specific portion of the member, **Bottle-shaped** strut is adopted to model the section, **Compression fan strut** emerges when stresses flow from a large source to a smaller source.

ACI 318R-19 [15] has been adopted for the analysis of the strut and tie model in this study. The strength of concrete in compression depends on the multi-axial state of stress and the disturbance from reinforcement and cracks. The effective compressive strength of the concrete strut is given in Eq. 1 as;

$$f_{ce}^{s} = 0.85 f_c' \beta_s \; or \; 0.67 f_{cu}' \beta_s \qquad (1)$$

$0.85 f_c'$ is the cylindrical concrete compressive strength and $0.67 f_{cu}'$ for the cube concrete compressive strength. β_s is the effective factor for concrete strut which accounts for the stress conditions, geometry and the crack angle surrounding the strut. The values of β_s for various conditions adopted for this investigation according to the ACI 318R-19, [15] is presented in Table 1. The tie cross section area, A_{st}, is taken as constant along its length and is obtained from the tie force and the yield stress of the steel, f_y. The nominal strength of a tie Ft is expressed in Eq. 2 as;

$$F_t = A_{st} f_y \qquad (2)$$

Table (1). Strut and Node Efficiency Factor According to ACI 318M-11

Strut and Node Efficiency	**Strut (β_s)**	**Node (β_n)**
Struts with uniform cross-section over its length	1.00	-
Bottle-shaped strut with reinforcement	0.75	-
Bottle-shaped strut without reinforcement	0.6	-
Struts in the tension member	0.4	-
All other cases	0.6	-
Nodal zone (C-C-C)	-	1.00
Nodal zone (C-C-T)	-	0.8
Nodal zone (C-T-T)	-	0.6
Nodal zone (T-T-T)	-	0.4

The compressive strength of concrete at the nodal zone depends on the tensile straining from tie intersection, confinement provided by compressive forces and the confinement by the transverse reinforcement. To distinguish between the confinement condition and straining for the nodal zone, Figure 2 presents the node classification.

- C-C-C is the nodal zone bounded by compression strut only,
- C-C-T is the nodal zone bounded by compression struts and a tension tie,
- C-T-T is the nodal zone bounded by a compression strut and two tension ties, and
- T-T-T is the nodal zone bounded by tension ties only.

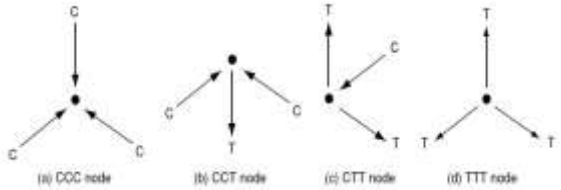

Figure (2): Nodes Classification

The effective compressive strength of concrete in a nodal zone, f_{ce}^{n}, is given in Eq. 3 as;

$$f_{ce}^{n} = 0.85 f_c' \beta_n \; or \; 0.67 f_{cu}' \beta_n \qquad (3)$$

β_n is the effectiveness strength factor of a nodal zone as given in Table 1.

The nominal compressive strength of a nodal zone, F_n, is given in Eq. 4 as;

$$F_n = f_{ce}^n A_z \quad (4)$$

A_z is the minimum of the area of the nodal zone where the force acts.

3. A numerical scheme for the beam verification

To determine the reinforcement for the simply supported deep beam in Figure 3, an assumed factored load of 2000kN was used, a concrete cylindrical strength, $f_c' = 30\ MPa$, steel yield stress $f_y = 400\ MPa$,

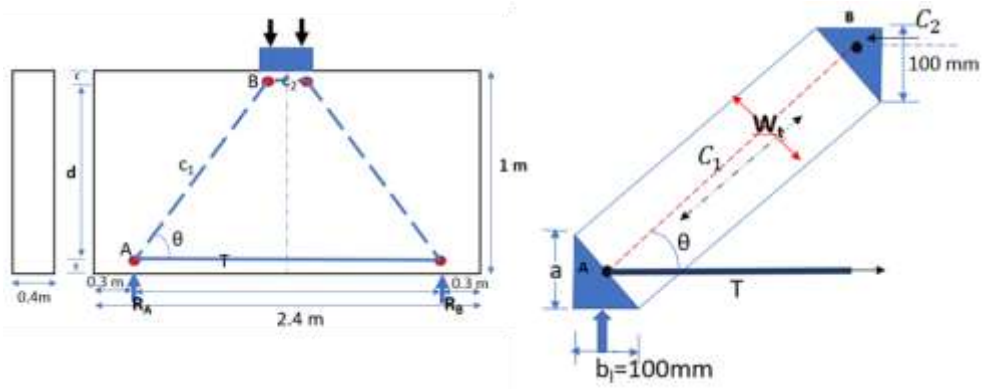

Figure (3): Beam dimension and strut and tie layout

A beam of 1m, a width of 400mm and the total length of 2.4 m were adopted. The beam self-weight is calculated as part of the applied load, the solution for the Strut and tie (STM) is given as;

The reaction regarding Figure 3, $R_A = R_B = 1000\ kN$

The shear span to depth ratio of this beam is less than 2, therefore, the beam is considered as the disturbed region (D region). Since the beam is symmetrical, the developed STM layout in Figure 3 consists of the strut in compression and the tie in tension. The width of the bearing plate is assumed as 200 mm, the upper nodes are usually located at a distance, c, equal one-quarter of the width of the bearing plate. Which is 50 mm. hence, the distance is assumed as 50mm.

The length of the diagonal strut C_1 is;

$$C_1 = \sqrt{(900^2 + 800^2)} = 1204.16\ mm$$

The force in strut $C_1 = 1000 \times \frac{1204.16}{900} = 1337.95\ kN$

The force in $T = 1000 \times \frac{800}{900} = 888.8\ kN$

$$C_2 = T = 888.8 kN$$

The angle between $C_1$and T, $\theta = tan^{-}\left(\frac{900}{800}\right) = 48.37^0$

3.1 Effective concrete design strength of struts and nodes

The effect of concrete design strength of the struts and nodes are calculated using the cylindrical concrete compressive strength as given in Eqs. 1 and 3 respectively.

The strut strength for the inclined strut $C_1$by adopting $\beta_s = 1$ for the bottle-shaped is;

$$f_{c1}^s = 0.85 f_c' \beta_s = 25.5\ MPa$$

The strut strength for the inclined strut $C_2$by adopting $\beta_s = 0.75$ for the prismatic shape is;

$$f_{c2}^s = 0.85 f_c' \beta_s = 19.125\ MPa$$

The effective design strength of the node using the cylindrical compressive strength for various nodes classification and adopting equivalent β_n in Table 1, can be calculated as;

At A, the node component is C-C-T thus,

$$f_{ce}^n = 0.85 f_c' \beta_n = 20.4\ MPa$$

At B, the node is C-C-C, $f_{ce}^n = 0.85 f_c' \beta_n = 25.5\ MPa$

The bearing stress generated from node B is given as

$$\frac{1000 \times 10^3}{100 \times 400} = 25\ MPa < f_{ce}^n\ 25.5 MPa \quad which\ is\ ok$$

For the section at the interface between strut C_2 and the node, the design strength should be the smaller of the node strength and the strut strength, both of which are the same in the case of 25.5 MPa.

The required width of strut C_2 is calculated as

$$w_{c_2} = \frac{F_{c_2}}{b \times f_{ce}^n} = \frac{888.8 \times 10^3}{400 \times 25.5} = 87.14\ mm$$

The difference between the assumed width of C_2=100 mm and the required width is on the safe side and is not significant, there is no need for dimension modification.

The required width for the strut C_1 is calculated as;

$$W_t = acos\theta + b_l sin\theta \quad (5)$$

$$W_t = 100sin48.37^0 + 100cos48.37^0 = 141.18\ mm$$

The corresponding stress is given as;

$$\sigma_{c_1} = \frac{F_{c_1}}{w_t \times b} \quad (6)$$

$$\sigma_{c_1} = \frac{1337.95}{141.18 \times 400} = 23.69 < f_{c1}^{s} = 25.5\ MPa, which\ is\ ok$$

The stress generated at node A is given as $\frac{1000\times10^3}{200\times400} = 12.5\ MPa < f_{ce}^{n} = 20.4\ MPa, which\ is\ ok$

3.2 Required Reinforcement

Since the strut joining nodes A and B has a bottle-shaped stress field, transverse reinforcement of the strut is required to resist a total force.

Strut C_1 requires transverse reinforcement as;

$$T_{c_1} = \left(\frac{1}{2} \times \frac{C_1}{2}\right) \times 2 = \frac{C_1}{2} = \frac{1337.95}{2} = 669\ kN$$

The total required reinforcement perpendicular to the strut is;

$$\frac{T_{c_1}}{f_y} = \frac{669\times10^3}{400} = 1672.44\ mm^2$$

The total length of C_1 is calculated as 1204.16 mm, hence the required transverse reinforcement is $\frac{1672.44}{1204.16} = 1.389\ mm^2/mm$, hence, a 10 mm diameter bar of 100 mm spacing is provided.

Tie T:

The reinforcement required to resist the force of this tie is;

$$\frac{T}{f_y} = \frac{888.8\times10^3}{400} = 2222\ mm^2$$

hence, $3Ø32\ of\ 2410\ mm^2$ is provided.

4. Finite Element Model and Loading

Three-dimensional nonlinear finite element model of the RC deep beam was adopted, the option is to present the hexagonal behavior of the nodes in an element. The meshing of the individual RC element has been achieved with the Concrete Model of 3-Dimension software package which allows the simulation of nonlinear response of concrete structures, the software allows the two materials (concrete and steel) to have a common node with a common element bonded together. The beam supports are made of elastic material which is simply supported. Figure 4 shows the model of the deep beam with the calculated reinforcing bar detailing. The model ensures proper bonding between the reinforcement and the concrete.

Table 2 shows the material strength properties of the concrete, reinforcement and the elastic support. Two kinds of loads; a static load at the top of the beam, was applied on each node with its magnitude calculated, and a pulsating load (this was applied by loading and unloading on each beam) as shown in Figure 4. The pulsating load was step-wisely applied on the nodes with the loading and unloading within 0.003 seconds, by adopting 5 time-step.

Numerical FEM investigation of the of the beam was carried out with the help of the Concrete Model of 3-Dimension. The beam was discretized into 894 elements, each element has the same dimension, and 1420 nodes.

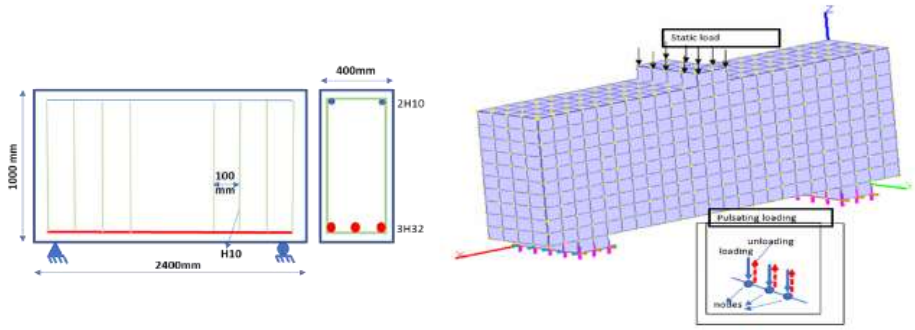

Figure (4): 3-dimensional FE model of Deep beam with rebar detailing

Table (2). Material Strength and Properties

Material property	***Concrete***	***Steel***	***Elastic Material***
Initial stiffness (MPa)	*2.2x10^5*	*2.1x10^6*	*2.2x10^6*
Poisson ratio	*0.2*	*0.3*	*0.3*
Unit weight (kN/m^3)	*25*	*78.6*	*78.6*
Yield strength (MPa)	-	*400*	-
Tensile strength (MPa)	*2.5*	*600*	-
Concrete Compressive strength (MPa)	*30*	-	-
Strain softening coefficient	*0.4 and 1.5*		

4.1. Cracks Delineation

The crack formed in the deep beam was evaluated in terms of the localized principal stresses and strains generated in the discretized critical element along the flexural cracks as expressed in Eqs. 7 and 8. Localized damage was evaluated using the combined stress-strain effect from the reinforced concrete element of the deep beam. Once the load reaches the ultimate value, the maximum yield strain is simultaneously reached hence further loading does not have an impact on the failure of the beam.

$$\sigma_d = \frac{(\sigma_x+\sigma_y)}{2} + \frac{1}{2}\sqrt{(\sigma_x-\sigma_y)^2+4\tau^2} \quad (7)$$

$$\varepsilon_d = \frac{(\varepsilon_x+\varepsilon_y)}{2} + \frac{1}{2}\sqrt{(\varepsilon_x-\varepsilon_y)^2+4\gamma^2} \quad (8)$$

- σ_d and ε_d are the diagonal tensile stress and the strain of in the reinforced concrete beam,
- σ_x and ε_x are the normal stress and strain,
- σ_y and ε_y are the orthogonal stress and strain to the corresponding normal stress and strain
- τ and γ are the shear stress and strain caused by the shear force along the corresponding normal and orthogonal stress-strain.

5. Global Damage Mode of the Deep beam

The failure mode of a deep beam is characterized by a deep inclined crack that appears to form within the shear span that does not depend on the flexural cracks. The cracks are initiated at the bottom of the beam near the support and propagate towards the face of the beam, Figure 5, this is cumulated with the compressive damage by the applied load at the region of the point load. The global damage forming a tied arch action. Such behavior has been linked to result from the stresses sustained by the tension bar transferred to crack concrete through bond effect at the ultimate state.

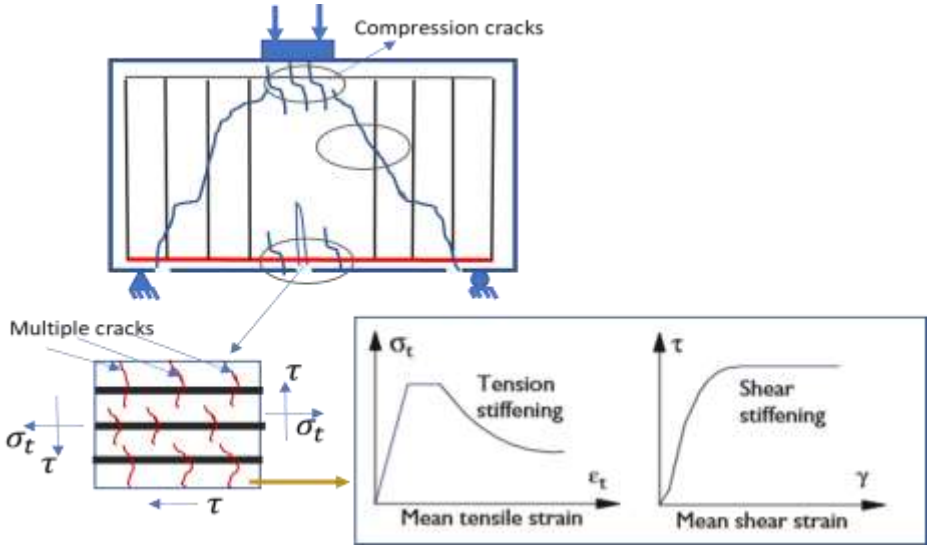

Figure (5): Damage Mode of Deep Beam

Figure 6 shows the principal strain of the damage mode of the beam when subjected to static load (left) and fixed-point pulsating load (right) at the midpoint. Concrete crack was initiated at an applied static load of about 350 kN at the bottom face of the beam close to the supports, while crack initiation for the fixed pulsating loads was around 195 kN equivalent to about 55 percent of the static load. Propagation of the cracks flows diagonally across the beam up to the compression zone forming a bottle-shape. Flexural crack was formed when the fixed pulsating load was applied as shown at the underside of the beam, this is due to the stepwise application of the pulsating load. Tension bar rupture leads to the rupture of the reinforcement at the compression zone in Figure 6 (right). Due to prolong loading, cracks of concrete were formed across all the stirrups and fracture occurred at least in the first two stirrups close to the supports. Rupture of stirrup close to the right support occurred at around a hundred thousand (100,000) cycles under the fixed pulsating loading accounting for a low strain less than 2000μ and total failure of the beam occurred at over 500,000 cycles.

Figure 7 shows the analytical response of the deep beam under the static and fixed-point pulsating load with the maximum capacity of 3360 kN and 3390 kN respectively which shows the same agreement. This increase to about 60% of the ultimate force, the curves exhibit an initial elastic relationship, with deviation from linearity at around 300 kN and 150 kN for the static and pulsating forces that correspond to the crack initiation phase. Crack propagation is symptomatic of increasing loading until the nonlinearity causes the variation in failure. Quasi-brittle failure of the concrete in both cases of the applied load is formed. Strain softening increases in the fixed pulsating case with larger deflection compared with the static case.

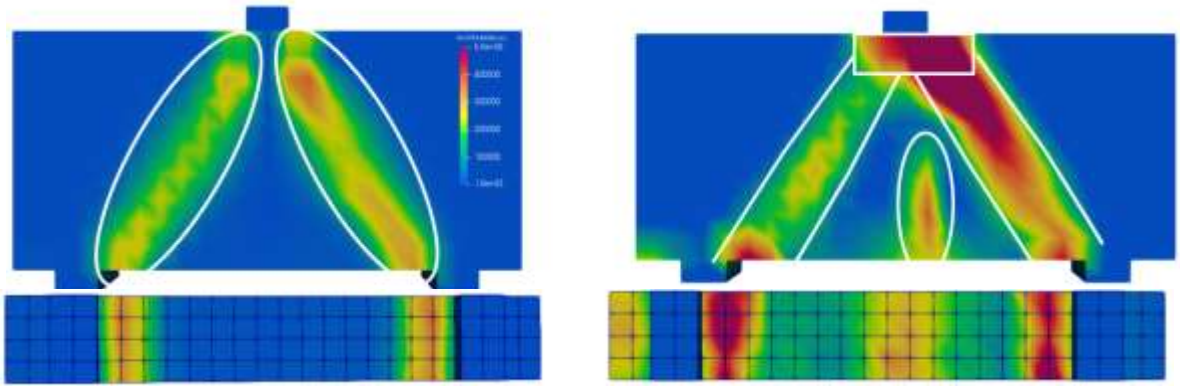

Figure (6): The principal strain of the Damage Mode of the Deep beam (a) Static point load (left) (b) Fixed-point Pulsating load (right).

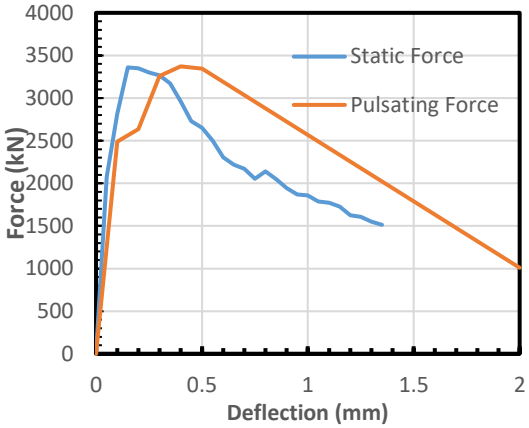

Figure (7): Load-Deflection Response of the beam the under pulsating loading

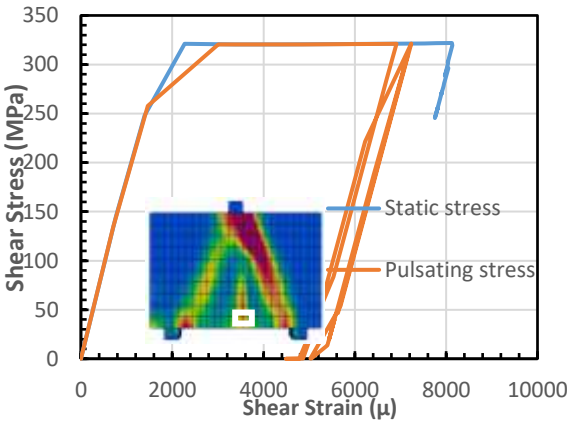

Figure (8): stress-strain comparison of the static and Static and Fixed Pulsating Load.

The softening properties of the stress-strain relation adopted in the constitutive model are mesh dependent which is defined by the finite element of the beam model; thus, similar meshes are used and are adjusted to eliminate the inconsistency in the fracture energy. The strain-softening coefficient in the plain concrete is considerably higher than the reinforced concrete element so that damage is delimitated by the total global failure of the material (see Table 2).

Figure 8 shows the stress-strain comparison of the static and the pulsating loads. A localized crack of the tensile element pickup as shown by a white rectangle was analyzed as discussed in section 4.1. there is an agreement between the static and the pulsating loading up to the proportional limit before deviation at stress over 250 MPa corresponding to strain 1600μ. There is an increase in strain at constant stress between the two curves after their corresponding yield strain before the failure of the static load. At the constant stress, the fixed pulsating load undergoes unloading and further reloading forming a loop around 7000μ strain which leads to loss of energy. Total failure formed by the curves is elasto-plastic fracturing.

6. Conclusion

Behavior of deep beam subjected to static and fixed pulsating load has been numerically analyzed using the strut and tie approach, the following conclusions are therefore reached.

1. The strut and tie model is efficient in calculating the various stresses generated in the beam, and hence reasonable estimate of the load carrying capacity of the analyzed reinforced concrete deep beam.
2. The 3-dimensional FE analysis of the normal strength concrete analyzed yielded an accurate anticipated response as deep beams are susceptible to shear damage. The shear failure occurred near the support and propagated up to the compression zone. Concrete crushing was observed at the loaded point in case of the applied fixed pulsating load, this occurred immediately before the shear crack grows towards the compression zone at about 500 thousand cycles.
3. The level of damage is higher under fixed pulsating loading when compared with static loading even at lower stress because of the stepwise loading of the beam, and as the concrete stress increases, the crack strength also increases.

7. References

[1] Lateef, H.T., Ibrahim, A.Q., "Human Error Uncertainties for Structural Detailing in Reinforced Concrete Buildings". Proceeding of School of

Engineering and Engineering Technology FUTA. pp. 766-779. August 2108.

[2] Ajibola, Q. I. (2019). "Reliability Appraisal of Nominal Eccentricity of Short Reinforced Concrete Column Designed to BS 8110 and Eurocode (EN:2)-Ultimate Limit State on Fatigue". Reliability Engineering and Resilience. https://doi.org/10.22115/rer.2019.197264.1013.

[3] Abdul-Razzaq, K. S., Jalil, A. M. & Jebur, S. F. Behaviour of reinforced concrete deep beams in previous studies. IOP Conf. Ser.: Mater. Sci. Eng. 518, 022065 (2019).

[4] Saleem Abdul-Razzaq, K. & Farhan Jebur, S. Suggesting alternatives for reinforced concrete deep beams by reinforcing struts and ties. MATEC Web Conf. 120, 01004 (2017).

[5] Zhi-Q.L., H., Zhao, H and Zhongguo J. M., Kim, T.H., Cheon, J.H., Shin., H.M., "Evaluation of behavior and strength of prestressed concrete deep beams using nonlinear analysis". Computers and Concrete 9, 63–79.

[6] Ritter, W., "Die bauweise hennebique (hennebiques construction method)." Schweizerische Bauzeitung (Zurich), 33(7), 59-61. 1899

[7] Mörsch, E., "Concrete Steel Construction (Der Eisenbetonbau). English Translation of the 3rd German Edition." McGraw-Hill Book Co., New York. 1909.

[8] Leonhardt, F., "Reducting the shear reinforcement in reinforced concrete beams and slabs". Magazine Concrete Research: 17(53): p187.December 1965,

[9] Rusch, H., "Researches toward a general flexural theory for structural concrete." Journal of ACI, 57(7), 1-27. 1960.

[10] Kupfer, H., "Erweiterung der Möhrsch'schen Fachwerkanalogie mit Hilfe des Prinzips vom Minimum der Formänderungsarbeit (Expansion of Mörsch's truss analogy by application of the principle of minimum strain energy)". CEB Bulletin: 40: Paris. 1964.

[11] Collins M. P. and Mitchell, D. "A rational approach for shear design-The 1984 Canadian code provisions, "ACI Journal 1986, 83(6), pp 925-933. 1986.

[12] Demerdash, W. E., El-Metwally, S. E., El-Zoughiby, M. E., and Ghaleb, A. A., "Strut-And-Tie Model and 3-D Nonlinear Finite Element Analysis for The Prediction of The Behavior of RC Shallow and Deep Beams with Openings," p. 21. 2014.

[13] Chen, W. F, and El-Metwally, S. E, "Understanding Structural Engineering from Theory to Practice". CRC Press, New York. 2011.

[14] Schlaich J., and Schafer, K., "Design and Detailing of Structural Concrete Using Strut-and- Tie Models". The Structural Engineering., V.69, No. 6, pp 113-125. 1991.

[15] ACI Committee 318-19 Building Code Requirements for Structural Concrete and Commentary.American Concrete Institute, 2019.